

# Generation of Passively Q-switched Fiber Laser using Different Erbium-Doped Fiber Absorption Coefficients

N. N. H. E. N. Mahmud<sup>a</sup> and N. A. Awang<sup>a</sup>

*<sup>a</sup>Optical Fiber Laser Technology (OPFLAT) Focus Group,  
Department of Physics and Chemistry, Faculty of  
Applied Sciences and Technology, Universiti Tun Hussein  
Onn Malaysia, 84600 Pagoh, Johor Malaysia.*

(Received: 2.6.21 ; Published: 4.4.22)

**Abstract.** This study demonstrated the performance of the passively Q-switched EDFL based on ITO-ZnO SA. By using different EDF absorption coefficients 6.43 dB/m (EDF M-5), 18.93 dB/m (EDF I-12), and 32.12 dB/m (EDF I-15) are compared in term of OSA spectrum, pulse width, and repetition rate. The setup is designed as a single ring cavity by employing an ITO-ZnO SA with a modulation depth of 21.01%, and ITO-ZnO saturates intensity at 0.089 MW/cm<sup>2</sup>. The experimental analysis result shows that the higher value of absorption coefficient EDF can give a stable Q-switched operation, but in the medium range of EDF absorption, absorption can give better pulse width and repetition rate results. ITO-ZNO SA is incorporated in a single ring configuration by comparing different EDF absorption coefficients for the first time. The pulse width and repetition rate for EDF M-5 are 5.95 μs and 40.07 kHz at 302.7 mW pump power. For EDF I-12, the pulse width and repetition rate are 4.35 μs and 40.96 kHz at pump power 302.7 mW. A repetition rate of 38.26 kHz for EDF I-15, is obtained at 302.7 mW with pulse width of 4.98 μs.

**Keywords:** Passively Q-switched, Erbium-doped fiber, Saturable absorber

## I. INTRODUCTION

Fiber lasers have various applications in fiber-optic communications, fiber optical sensing, micromachining, and spectroscopy [1-2]. A Q-switched laser is typically realized by active or passive technique. In terms of the fiber laser cavity, passive Q-switched techniques are more attractive due to compactness, simplicity, and flexibility than active techniques. Passive Q-switched pulsed can be achieved by insertion of saturable absorber (SA) in the cavity design via sandwiching it between fiber ferrules. In the past two decades, different types of SA have been implemented, such as semiconductor saturable absorption mirror (SESAM), graphene, graphite. Initially, a semiconductor material such as a semiconductor saturable absorber mirror (SESAM) is the first method used to generate pulse Q-switched [3]. However, a SESAM often has drawbacks, such as a narrow working bandwidth and a time-consuming fabrication process limiting pulse generation [4].

Another type of SA material is carbon allotrope (graphene, graphite, carbon nanotube), transition metal oxide (zinc oxide), transparent conducting oxides (TCOs) such as indium tin oxides, ITO, and topological insulator (bismuth diselenide). However, most of these materials suffer from limitations; hence surge for efficient materials as SA is still relevant.

Transparent conductive oxide (TCO), acting as a thin film, has been widely used as a transparent electrode due to its unique characteristics of TCO with the high optical transmission, electrical conductivity, and broadband gap of around 3.5 eV [5]. Other researchers reported that ITO can be seen as a potential SA candidate because it enables a wide range of saturable absorption due to the position of the plasmonic absorption peak of ITO can be varied from 1600 nm to 2200 nm by controlling the concentration of tin doping. The plasmon frequency of ITO lies in the NIR because the carrier density is much lower than most conductive oxides. This allows the ITO to have a strong plasmonic absorption peak with wide bandwidth [6]. Not only that, ITO can acquire a fast and extensive intensity-dependent refractive index and has a rapid recovery time of around 360 fs.

Since 1960, ZnO has gained so much attention due to its various applications, such as sensors, transducers, and catalysts [7]. Aneesh et al. reported that zinc oxide (ZnO) is an alternative SA since this material has a unique characteristic, such as large excitation binding energy of 60 meV with a direct bandgap of 3.37 eV [8]. ZnO is a group II-IV compound semiconductor with its covalence on the borderline between ionic and covalent semiconductors. It has a hexagonal wurtzite structure showing a partial polar. For the most part, ZnO is widely used in optoelectronic devices due to its ability to withstand large electric fields, high power operation, and high-temperature properties [9-10].

To our knowledge, we first demonstrated that the ITO-ZnO thin film could be used as SAs for a pulsed fiber laser. SA was integrated into the laser cavity by sandwiching the ITO-ZnO SA between two fiber ferrules with a fiber connector. A stable Q-switched pulse at a pump power of 302.7 mW is observed by comparing 3 EDF absorption coefficients. The result shows that EDF I-12 represents a good sign for Q-switched fiber laser because of its narrower pulse width and higher repetition rate than the others.

## **II. INDIUM TIN OXIDE-ZINC OXIDE AS SATURABLE ABSORBER**

The preparation of saturable absorber using mechanical exfoliation process of ITO-ZnO was on the fiber ferrules tip. The fiber ferrule is made of two types of materials zirconia ceramic or composite plastic polymers. Both ceramic and composite ferrules provide excellent optical performance, with an average insertion loss of 0.3dB. Before the deposition process, the fiber ferrules tip was cleaned with fiber cleaner, which is isopropyl alcohol. The fiber ferrule should be cleaned with a figure of 8 wiping action to prevent scratches. The cleaned fiber ferrules were then observed by using fiberscope, FS201 Thorlabs, to make sure fiber ferrules were free from dust and fingerprint. The cleaning steps need to be repeated if the surfaces are not adequately cleaned. After the cleaning process, the ITO-ZnO was exfoliated by using a glass slide, as shown in Figure 1. The exfoliation process of ITO-ZnO on the fiber ferrules was used for the passively Q-switched generation.

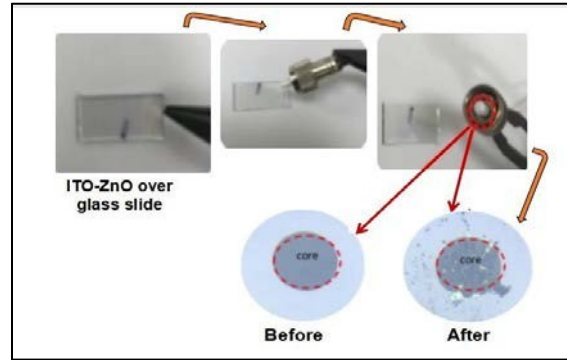


FIGURE 1. Mechanical exfoliation process.

### *Nonlinear Absorption properties of ITO-ZnO Saturable Absorber*

ITO-ZnO was characterized by twin detector methods to measure nonlinear absorption such as modulation depth, saturation intensity, and absorption of non-saturable absorption graphs, as shown in Figure 2. The mode-locked pulse seed that has been used as a source can operate at a central wavelength of 1563 nm and has a repetition rate of 12.64 MHz with a pulse width of 716.5 fs. The mode-locked pulse is connected to the attenuator before being split up by a 3 dB coupler. The ITO-ZnO SA was attached at one of the output couplers ports. Another port of output coupler was joined to OPM designated as a reference signal. The modulation depth of the ITO- ZnO is stated as a percentage of the linear absorption due to the normalization, as shown in Equation 1:

$$\alpha(I) = \frac{\alpha_s}{1 + \frac{I}{I_s}} + \alpha_{ns} \quad (1)$$

where  $\alpha(I)$  is the absorption coefficient  $\alpha_s$  and  $\alpha_{ns}$  are saturable absorption and non-saturable absorption,  $I$  is the intensity and  $I_{sat}$  is saturation intensity. Figure 3 shows the graph of the nonlinear absorption of ITO-ZnO deposited onto the fiber ferrules. The graph displays the nonlinear absorption of ITO-ZnO with a modulation depth of 21.01% and saturation intensity of  $0.089 \text{ MW/cm}^2$ . Generally, stable pulsed fiber laser operation will have a high modulation depth that is greater than 10% [11-13]. High modulation depths usually lead to a greater nonlinear absorption that periodically increases insertion loss and reduces laser performance. Therefore, the saturable absorption needs to be controlled [14-16]. Higher SA modulation depth may suggest better recovery capabilities and single pulsating generation stabilization [17]. As the power of the pump increases, the gain signal increases due to the generation of Q- switching depends on the level of saturation of the SA [18].

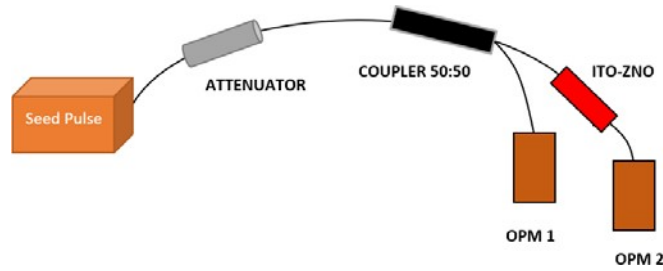


FIGURE 2. Nonlinear saturable absorption of ITO-ZnO measurement setup.

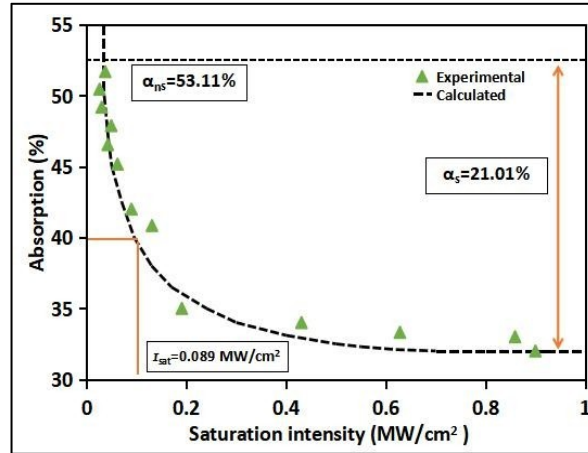


FIGURE 3. The nonlinear absorption of ITO-ZnO SA.

### Single ring Fiber Laser based on ITO-ZnO Saturable Absorber

The single ring cavity consists of 3 m EDF, which has three different absorption coefficients, which are 6.43 dB/m, 18.93 dB/m, and 32.81 dB/m. The experiment was set up with a gain medium which is erbium-doped fiber (EDF) with different EDF absorption coefficients of 6.43 dB/m (EDF M-5), 18.93 dB/m (EDF I-12), and 32.12 dB/m (EDF I-15). Meanwhile, EDF acts as an optical amplifier that uses the active erbium-doped fiber and pumps source (signal or laser) to boost or amplify the optical signal in the cavity. A 980 nm laser diode was used to pump EDF via wavelength division multiplexing (WDM). This cavity was set up by inserting an ITO-ZnO as a saturable absorber. The ITO-ZnO SA was placed between the isolator and 90:10 optical coupler, as shown in Figure 4. Optical isolator input signals were used to ensure a unidirectional signal in the ring cavity, so the output of 90% OC oscillated backward in the cavity [19]. The remaining 10% of signal output was connected through another 50:50 OC. Two 50:50 OC ports were used to transmit the output spectra displayed by OSA with a resolution of 1.0 nm and repetition rate by the oscilloscope (OSC). The total ring cavity of this setup is 7.44 m. All fiber components were spliced to each other. Configuration of passively Q-switched fiber laser was the same as all EDFs.

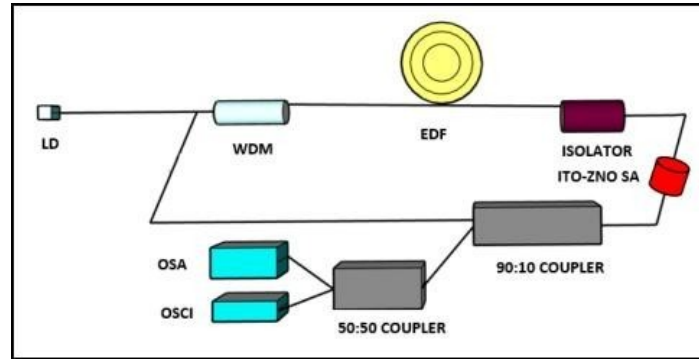


FIGURE 4. Experimental setup of passively Q-switched fiber laser.

### III. RESULT AND DISCUSSION

The proposed single ring is represented by different EDF absorption coefficients: low, medium, and high. Figure 4 shows the OSA spectrum of passively Q-switched EDFL incorporating ITO-ZnO SA. This cavity is observed to have a Q-switching threshold at a pump power of 153.4 mW for all EDFs. At a maximum pump power of 302.7 mW, the output power obtained for EDF M-5, EDF I-12, and EDF I-15 is -3.43 dBm, -5.63 dBm, -6.32 dBm, respectively, as shown in Figure 5. The spectral bandwidth for each EDF is 0.6 nm, 1.8 nm, and 1.25 nm. This is because the spectral bandwidth is directly influenced by the high absorption coefficient of EDF used. The spectral bandwidth can be generated by calculating the gain of EDF. The gain is proportional to the absorption coefficient of the EDF, and more significant absorption raises the gain value. The EDF is also homogeneous, broadening the spectrum range due to energy splitting into several sub-levels related to the thermalization effect. The form of the atomic linewidth transition was created using Lorentzian theory. As a result, if the cavity and surrounds supply the necessary conditions, the atomic transition exhibits the same line shape [20]. The gain coefficient  $\gamma\gamma(\nu)$  of Lorentzian can be obtained by:

$$\gamma\gamma(\nu) = \gamma(\nu_0) \frac{\left(\frac{\Delta\nu}{2}\right)^2}{(\nu - \nu_0)^2 + (\Delta\nu/2)^2} \quad (2)$$

where  $\gamma(\nu_0)$  is defined as the gain coefficient at a central frequency, while  $\nu_0$  and  $\Delta\nu$  are described as the emission linewidth.

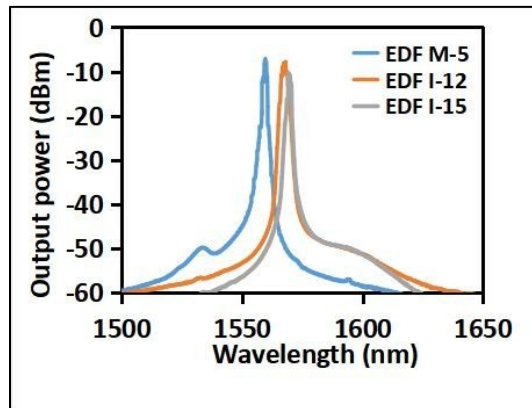


FIGURE 5. The optical spectrum for EDF M-5, EDF I-12 and EDF I-15.

Figure 6 provides the pulse train obtained for EDF-M-5, EDF I-12, and EDF I-15 using an oscilloscope. Each EDF shows pulse duration of 24.96  $\mu\text{s}$ , 24.41  $\mu\text{s}$ , and 26.14  $\mu\text{s}$  which corresponded to a repetition rate of 40.07 kHz, 40.96 kHz, and 38.26 kHz, respectively. The EDF I-12 shows the shortest pulse duration than EDF M-5 and EDF I-12. This is due to the pump power and gains applied for EDF I-12 being sufficient to give the shortest pulse [21].

From the output pulse train graph, the pulse width of EDF I-12 is 4.35  $\mu\text{s}$ , which shows a narrower pulse width than others. However, the EDF I-15 shows a pulse width of 4.98  $\mu\text{s}$  which is broader than EDF I-12. This observation indicates that erbium ion with high absorption coefficients is still insufficient to generate the highest repetition rate with short pulse width. Based on the previous research, erbium ions also depend on the optimum length used. As the density of erbium ion increases, the optimum length decreases, which is suitable for clumping amplifiers due to the high concentration of erbium ion, which damages the gain due to the clustering. This effect is known as cooperative energy transfer (CET), which reduces the lifespan of the fluorescent [22]. Therefore, when the EDF absorption coefficients are higher, it cannot guarantee that the Q-switched pulse is stable because the optimum length of EDF must be taken into account, as erbium ions increase when the optimum length decreases.

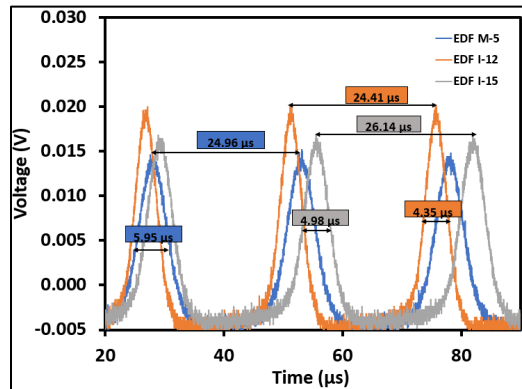


FIGURE 6. The pulse train of passively Q-switched EDFL for EDF M-5, EDF I-12 and EDF I-15.

The fundamental frequency is used to characterize the stability of the passively Q-switched EDFL pulse operation in the frequency domain as plotted in Figure 7 (a), (b) & (c). The fundamental frequency of three EDF at a pump power of 302.7 mW generates SMSR values of 32.30 dB, 32.60 dB, and 31.50 dB. The graph shows the highest SMSR value of 32.60 dB for EDF I-12. Based on Tan [23], the stability of passively Q-switched fiber laser can be obtained by the highest SMSR value. Therefore, the higher pump power applied can generate a higher value of SMSR. Meanwhile, the SMSR value depends not only on the pump power but also on the EDF absorption coefficients used due to the value for EDF I-15 showing the smallest SMSR value. The EDF-I-12 with medium absorption coefficients attained the highest SMSR value as compared to EDF M-5 and EDF-I-15.

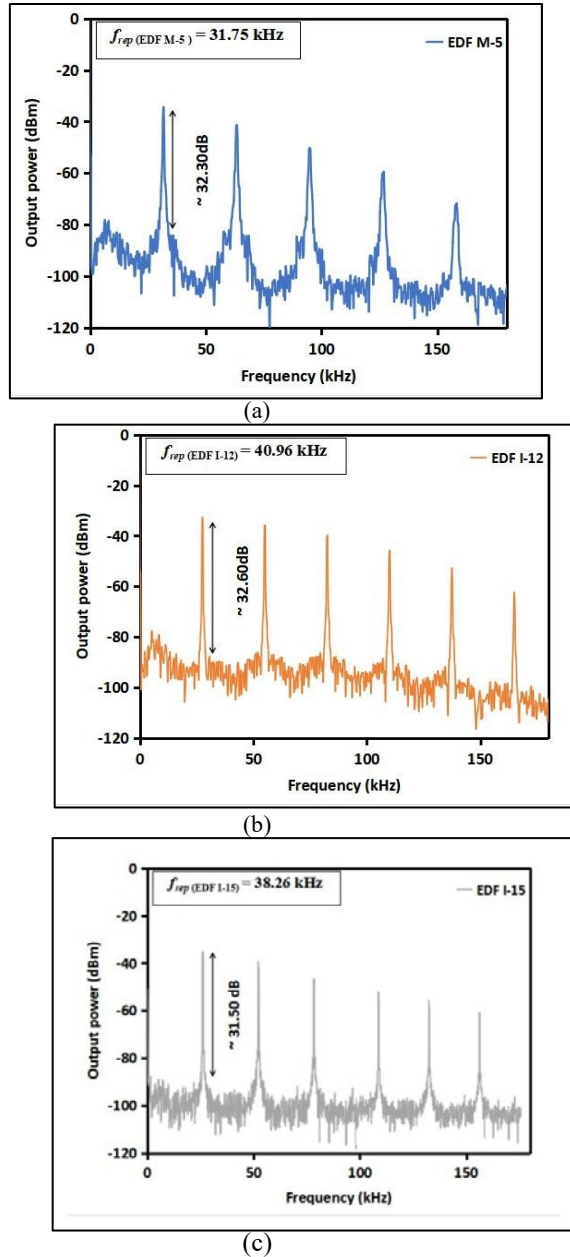


Figure 7: The fundamental frequency of (a) EDF M-5 (b) EDF I-12 (c) EDF I-15

Table 1 shows three EDF absorption coefficients that produce passively Q-switched EDFs. The output power of EDF M-5 is greater than EDF I-12 and I-15 due to the different concentrations of erbium ions used. However, EDF I-12 provides broader spectral bandwidth than other EDFs due to the population inversion and spectral broadening based on self-phase modulation (SPM). Not only that, it is shown that the gain increases with an increasing numerical aperture (NA) and remains constant after a certain level for each pump power; the purpose for this is that the amplifier reaches the population inversion. This proves that the gain increases when NA increases because larger NA indicates an overlap between the optical mode field and the erbium ion [22]. Moreover, the required NA to obtain maximum gain with increasing pump power becomes less. Thus, it produces a stable passively Q-switched

EDFLs same as EDF I-12, which have a higher repetition rate and smaller pulse width due to the EDF's suitable NA and optimum EDF length at 18.93 dB/m of absorption coefficients. In conclusion, the passively Q-switched EDFL is influenced by optimum length, NA, EDF absorption coefficients and requires suitable pump power to generate good performance of Q-switched.

**Table 1.** Comparison performance of the passively Q-switched EDFL at different absorption coefficients.

	EDF M-5	EDF I-12	EDF I-15
EDF Absorption Coeff.(dB/m)	6.43	18.93	32.12
Pump Power (mW)	302.7	302.7	302.7
Threshold Pump Power (mW)	153.4	153.4	153.4
Output Power (dBm)	-3.43	-5.63	-6.32
Spectral Bandwidth(nm)	0.6	1.8	1.25
Pulse Width ( $\mu$ s)	5.95	4.35	4.98
Pulse Duration( $\mu$ s)	24.96	24.41	26.14
Repetition rate (kHz)	31.75	40.96	38.26
SMSR (dB)	32.30	32.60	31.50
Numerical Aperture	0.23	0.24	0.25

#### IV. CONCLUSION

In this work, we demonstrated the passively Q-switched EDFL based on ITO-ZnO SA in output power, pulse width, repetition rate, side-mode suppression ratio (SMSR), and spectral bandwidth by using three different absorption methods coefficients. The three EDF M-5, EDF I-12, and EDF I-15 decrease output power when pumping power increases. However, the Q-switching operation for EDF I-12 obtained a good sign in Q-switched pulse compared to EDF M-5 and EDF I-15 due to the SA, optimum length EDF, a numerical aperture of EDF utilized inside the laser cavity. As the erbium ion increases, optimum length EDF decreases, resulting in the gain signal increases. Meanwhile, when the pump power increases, the gain signal increases depending on the level of saturation SA, affecting the laser performance of Q-switched. Thus, the stable passively Q-switched EDFL is influenced by the properties of the EDF and the SA material used to generate a higher repetition rate and narrower pulse width.

#### ACKNOWLEDGMENTS

The authors acknowledge Ministry of Higher Education (MOHE) through Fundamental

Research Grant Scheme (FRGS) (FRGS/1/2019/WAB05/UTHM/02/5) (grant No: K170) and Research Management Centre (RMC) of University Tun Hussein Onn Malaysia for supporting this FRGS VOT K170.

## REFERENCES

1. O. Okhotnikov, A. Grudinin, M. Pessa, Ultra-fast fibre laser systems based on SESAM technology: new horizons and applications. *New J.Phys*, 6: 22 (2004).
2. U. Keller, Recent developments in compact ultrafast lasers, *Nature* 424, 831–838 (2003).
3. S. W. Harun, M. A. Ismail, F. Ahmad, M. F. Ismail, R. M. Nor, N. R. Zulkepali and H. Ahmad, A Q-switched erbium-doped fiber laser with a carbon nanotube based saturable absorber. *Chinese Physic Letter*, 29(11) (2012).
4. K. Zhang, M. Feng, Y. Ren, X. Cheng, J. Yang and J. Tian, Q-switched and mode-locked Er- doped fiber laser using PtSe<sub>2</sub> as a saturable absorber. *Photonics Research*, 6(9), 893-899 (2018).
5. N. U. H. H. Zalkepali, N. A. Awang., Y. R. Yuzaile, Z. Zakaria, A. H. Ali and N. N. H. E. N. Mahmud, Tunable indium tin oxide thin film as saturable absorber for generation of passively Q- switched pulse erbium-doped fiber laser. *Indian Journal of Physics*, 1-7 (2020).
6. G. V. Naik, V. M. Shalaev, A. Boltaseva, A. Alternative plasmonic materials: beyond gold and silver. *Adv Mater*, 25:3264–94 (2013)
7. Z. L. Wang, Zinc oxide nanostructures: growth, properties and applications, *J. Phys.: Condens.Matter* 16, R829–R858 (2004).
8. P. M. Aneesh, K. A. Vanaja and M. K. Jayaraj, Synthesis of ZnO nanoparticles by hydrothermal method, *Nanophotonic Mater: IV*, vol. 6639, 2007, pp. 66390J.
9. A. N. Madathil, K. A. Vanaja, M. K. Jayaraj, Synthesis of ZnO nanoparticles by hydrothermal method. *Proc of SPIE*, pp. 6639: 1–9 (2007).
10. H. Ahmad, C. S. J. Lee, M. A. Ismail, Z. A. Ali, S. A. Reduan, N. E. Ruslan and S. W. Harun, Zinc oxide (ZnO) nanoparticles as saturable absorber in passively Q-switched fiber laser. *Optics Communications*, 381, 72-76 (2016).
11. O. Svelto, and D. C. Hanna, Principles of lasers (Vol. 4). New York: Plenum press. 1998.
12. H. Ahmad, S. A. Reduan, A. S. Sharbirin, M. F. Ismail and M. Z. Zulkifli, Q-switched thulium/holmium fiber laser with gallium selenide. *Optik*, 175: 87-92 (2018).
13. K. Y. Lau, N. Z. Abidin, M. A. Bakar, A. A. Latif, F. D. Muhammad, N. M. Huang and M. A. Mahdi, Passively mode-locked ultrashort pulse fiber laser incorporating multi-layered graphene nanoplatelets saturable absorber. *Journal of Physics Communications*, 2(7): 075005 (2018).
14. Q. Bao, H. Zhang, J. X. Yang, S. Wang, D. Y. Tang, R. Jose and K. P. Loh, Graphene–polymer nanofiber membrane for ultrafast photonics. *Advanced functional materials*, 20(5): 782-791 (2010).
15. Z. Luo, M. Zhou, J. Weng, G. Huang, H. Xu, C. Ye and Z. Cai, Graphene-based

- passively Q-switched dual-wavelength erbium-doped fiber laser. *Optics letters*, 35(21): 3709-3711 (2010).
16. J. Ma, G. O. Xie, P. Lv, W. L. Gao, P. Yuan, L. J. Qian and D. Y. Tang, Graphene mode-locked femtosecond laser at 2  $\mu\text{m}$  wavelength. *Optics letters*, 37(11): 2085-2087 (2012).
  17. A. G. Rozhin, Y. Sakakibara, S. Namiki, M. Tokumoto, H. Kataura, & Y. Achiba, Sub-200-fs pulsed erbium-doped-fiber laser using a carbon nanotube-polyvinylalcohol mode locker. *Applied physics letters*, 2016. 88(5):051118.
  18. H. Ahmad, M. J. Faruki, M. Z. A. Razak, M. F. Jaddoa, S. R. Azzuhri, M. T. Rahman, & M. F. Ismail, A combination of tapered fibre and polarization controller in generation highly stable and tunable dual-wavelength C-band laser. *Journal of Modern Optics*. 2017. 64(7):709-715.
  19. K. Y. Lau, F. D. Muhammad, A. A. Latif, M. H. A. Bakar, Z. Yusoff, & M. A. Mahdi, Passively mode-locked soliton femtosecond pulses employing graphene saturable absorber. *Opt. Laser Technol*, 2017. pp. 221–227.
  20. H. Y. Ryu, W. K. Lee, H. S. Moon, & H. S. Suh, Tunable erbium-doped fiber ring laser for application of infrared absorption spectroscopy. *Optics communication*. 2007. 275(2): 379-384.
  21. S. W. Harun, H. Ahmad, M. A. Ismail and F. Ahmad, Q-switched and soliton pulses generation based on carbon nanotubes saturable absorber. In *2013 Saudi International Electronics, Communications and Photonics Conference* (pp. 1-4). IEEE. 17 92013).
  22. E. Desurvire, J. L. Zyskind, & C. R. Giles, Design optimization for efficient erbium-doped fiber amplifiers. *Journal of lightwave technology*, 1990. 8(11), 1730-1741.
  23. S. J. Tan, S. W. Harun, N. M. Ali, M. A. Ismail and H. A. Ahmad, A multi-wavelength Brillouin erbium fiber laser with double Brillouin frequency spacing and Q-switching characteristics. *IEEE Journal of Quantum Electronics*, 49(7): 595-598 (2013).